Supplemental Data

Methods

PBMCs isolation and cryopreservation

Venous blood was collected in sodium heparin BD Vacutainers and transported at room temperature to the KEMRI research center laboratory (time of transport 20 mins by road). Absolute lymphocyte counts were determined from whole blood using BC-3000 Plus Auto Hematology Analyzer, 19-parameters (Shenzhen Mindray Bio-Medical Electronics Co.). Peripheral blood mononuclear cells (PBMCs) were isolated within 2 hours after collection using Ficoll-Hypaque density gradient centrifugation. After two washes with PBS, cells were counted using Trypan Blue staining and hemocytometer by microscopy. Average yield from all children included in this study was 2 million PBMCs per ml whole blood. Cells were frozen at $5x10^6$ cells/ml in freezing medium comprising 90% heat-inactivated, filter-sterilized fetal bovine serum and 10% dimethyl sulfoxide (Sigma) using Mr Frosty™ freezing container overnight at -80^0C. PBMCs were transferred to liquid nitrogen storage until use. PBMCs were also collected and isolated following the same process, from healthy adult donors from the United States of America (N=6) and used as controls for NK phenotype and functions, for each experiment.

Thawing samples

PBMCs were thawed and diluted with 15 times the sample volume with 37^0C complete media (RPMI 1640, GIBCO with 10% heat-inactivated and filter-sterilized fetal bovine serum, Glutamine 1X GIBCO, Penicillin/Streptomycin 1X GIBCO, Hepes BioWhittaker 17-737E 10mM). Cells were washed twice with the same media, spinning for 12 mins centrifugation at 250g. Live cells were counted using Propidium Iodide and MACSquant Flow cytometer or cell counter. Cells were either stained immediately or cultured for 6 hours following experimental protocols below.

Flow cytometry phenotyping

Based on methods published by the G. Alter laboratory [1], we used 4 multicolor panels to assess NK marker expression for PBMCs collected from Kenyan children. For each panel we used a

dump channel with anti-CD3 (BD and Biolegend, clone UCHT1), anti-CD14 (Invitrogen and Biolegend, TüK4) antibodies and live/dead staining (Life technology, Violet L/D). NK cell subsets were identified using anti-CD56 (BD, NCAM16.2) and anti-CD16-BV510 (Biolegend, 3G8) antibodies. The first panel measured KIRs expression: anti-KIR2DL1/KIR2DS5-FITC (R&D, #143211), anti-KIR2DL3/CD158b2-APC (R&D, #180701), anti-KIR2DL1/KIR2DS1-PECy7 (Beckman Coulter, EB6B), anti-KIR2DL2/DL3-PE (Miltenyi, DX27), anti-KIR3DL1-BV421 (Biolegend, DX9) antibodies. The second panel covered the NKG2 family: NKG2A-PE (Beckman Coulter, Z199), NKG2C-BUV395 (biotin Miltenyi, REA205/streptavidin-BUV395 BD), NKG2D-APC (BD, 1D11), CD94-FITC (BD, HP-3D9), CD57-Pacific Blue (Biolegend, HCD57) antibodies. The third panel included anti-NKp30-AF647 (BD, p30-15), NKp46-PE (BD, 9E2/Nkp46), 2B4-FITC (BD, 2-69). The fourth panel used anti-CD160-AF647 (Biolegend, By55), anti-CD161-FITC (Miltenyi, 191B8), anti-TRAIL-PE (Biolegend, RIK-2), anti-Perforin-PerCPeF710 (Affymetrix, d9G) antibodies. The first three panels were fixed using 4% PFA and the fourth panel using cytofix/cytoperm (BD); 1 to 1.5 million cells were stained per panel.

Data was acquired with an average of 245,074 and a median of 234,269 lymphocytes gated on FSC/SSC cytogram [range: 115,414 to 332,155] (see supplemental figure 2A for gating strategy), on an LSRII flow cytometer 5 lasers (UMMS Flow Core Facility) using compensation and FMO controls. Using Live/Dead staining, we obtained an average of 78.39% live lymphocytes for all the samples ran (median 78%; range from 71.8% to 86.0%). Data were analyzed with Flow-Jo software, version 10.1r5 and GraphPad Prism software, version 7.0a.

NK cells functional assay

Thawed PBMCs (10^6) were incubated at 37^0C with 5%CO_2, in same complete media as described above for 6 hours with anti-CD107a-PECy5 antibody (BD, H4A3), Golgi STOP (BD, 0.7µl/ml), Golgi PLUG (BD, 1µl/ml) and the K562 cell lines (400k/ml, cell line from Kim Dohoon's laboratory, University of Massachusetts) or with complete media (unstimulated) as a negative control. Cells were then stained using extracellular (CD3/CD14/CD56/CD16, described above) and intracellular markers: anti-MIP-1β-PE (BD, D21-1351), anti-TNF-α-AF700 (BD,

Mab11) and anti-IFN-γ-FITC (BD, 25723.11) antibodies. Permeabilization was performed with cytofix/cytoperm (BD).

Data was acquired with an average of 345,408 and a median of 216,624 lymphocytes gated on FSC/SSC cytogram, [range: 102,277 to 553,500], (see supplemental figure 2A), on an LSRII flow cytometer 5 lasers (UMMS Flow Core Facility) using compensation and FMO controls. Using Live/Dead staining, we obtained an average of 78.73% live lymphocytes for all the samples ran (median 83.9%; range 76.45% to 88.23%). Data were analyzed with Flow-Jo software, version 10.1r5 and GraphPad Prism software, version 7.0a.

EBV load

EBV load was measured by quantitative Polymerase Chain Reaction (qPCR), as previously described [2–4]. DNA was extracted from PBMCs using the Qiagen DNA easy kit (Qiagen) following the manufacturer's instructions and stored at -20^{0}C until use. The eBL group was divided into 2 subgroups based on EBV status: no or low EBV loads detected in peripheral blood and high EBV copy numbers (>3 log EBV copies/µg of DNA). This cut-off was determined previously by the threshold observed between Kisumu and eBL children [4].

Determination of IgG antibody levels in Human Sera

Luminex multiplex, bead-based assay was used to detect antibodies as described elsewhere [5–7]. Four synthetic peptides covering immunodominant epitopes of VCA P18, ZEBRA, EAd-p501 and EBV nuclear antigen 1 (EBNA1) were used to determine EBV sero-positivity (gift from Jaap Middeldorp). CMV antibodies were measured to a native pp65 CMV antigen (strain AD169) produced in MRC-5 cells (from East Coast Bio, Part/Lot: LA209-V2181). History of cumulative malaria exposure was determined using a malaria serology profile consisting of recombinant peptides to liver and blood stage malaria antigens: AMA1, MSP1, CelTos (gift from Sheetji Dutta, Evelina Angov and Elke Bergmann from the Walter Reed Army Institute of Research) and r*Pf*-SEA-1A (described in [8]), r*Pf*-GARP (gift from Jonathan Kurtis at Brown University, RI).

To measure IgG antibody levels in our human sera samples, we used a bead-based assay developed from published methods [9]. Specifically, 200µg of each antigen (ThermoFisher Scientific) or BSA (Sigma) in 50mM MES, pH5.0 was amine coupled to $1.25x10^7$ microspheres (Luminex). Antigen-coated beads were incubated with human plasma samples at 1:100 for one hour at 25^0C in Assay Buffer E (ABE, PBS pH7.4 containing 0.1% BSA, 0.05% Tween-20, and 0.05% sodium azide) in microtiter filter bottom plates (Millipore). Microspheres were washed three times in ABE by vacuum filtration and incubated for 1 hour at 25^0C with biotinylated anti-human IgG (Pharmingen) diluted 1:1000 in ABE. Microspheres were washed three times in ABE by vacuum filtration and incubated at 25^0C with phycoerythrin conjugated streptavidin (Pharmingen) diluted 1:1000 in ABE for 15 minutes. Microspheres were washed a final three times in ABE by vacuum filtration and resuspended in 125µL ABE. Antigen-specific fluorescence values were quantified on a BioPlex 200 multi-analyte analyzer with subtraction of fluorescence values obtained with BSA-conjugated beads. Results are reported as mean fluorescent intensity (MFI) after acquisition of minimum 50 beads.

Statistics:

For the categorical data (sex and viral load variables between our groups) we used Chi^2 statistical test. For the numerical data and based on the low sample size of each groups (Nandi n=7; Kisumu n=7 and eBL n=14) we used non-parametric statistical test: one way Kruskal-Wallis (KW), Mann-Whitney *t* test (MW) two-tailed or Wilcoxon *t* test two-tailed using GraphPad Prism software, version 7.0a. Results are expressed using the median and *p*-value. When $p>0.05$ the result was indicated non-significant (n.s) otherwise we used the following symbols: *$p<0.05$; **$p<0.01$; ***$p<0.001$ and ****$p<0.0001$.

Supplemental Figures

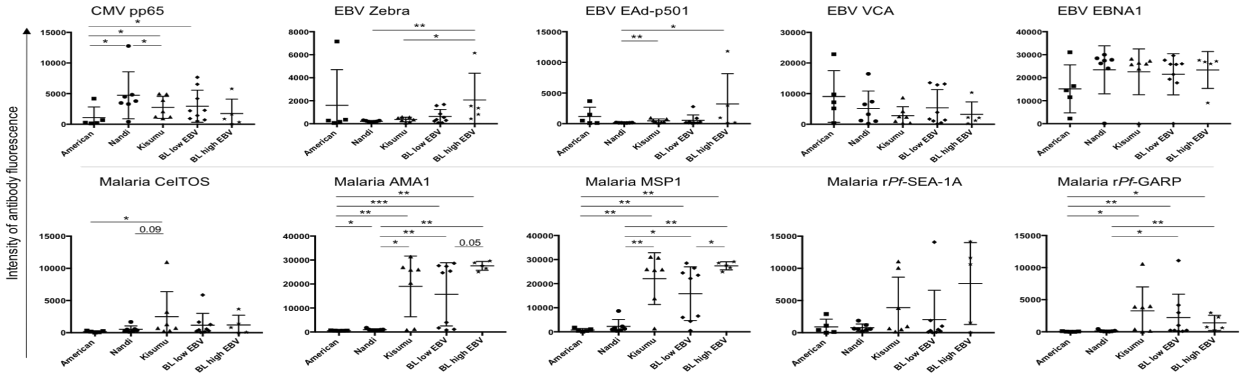

Figure S1: Antibody levels to malaria, EBV and CMV within our study populations. The mean fluorescent intensity (MFI) of IgG antibodies to the following antigens: pp65 for CMV; Zebra, EAd-p501, VCA and EBNA1 from EBV, and CelTOS, AMA1, MSP1, r*Pf*-SEA-1A and r*Pf*-GARP from malaria. (n.s = non-significant; *p<0.05; **p<0.01; ***p<0.001). Study populations included North American malaria-naive controls (n= x), Nandi (n=x), Kisumu (n=x) children and eBL patients from Kenya with low EBV (n=x) and high EBV (n=x) peripheral blood levels.

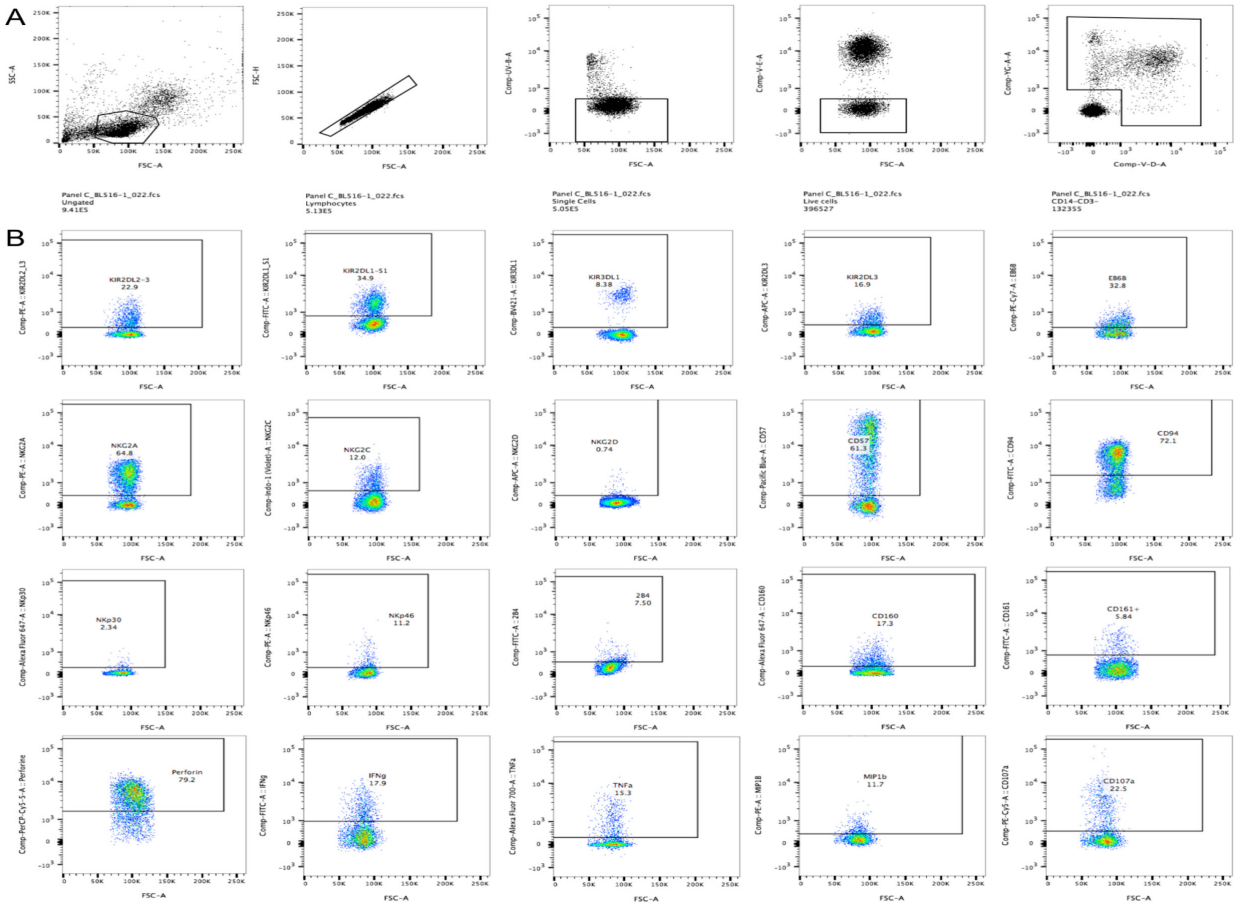

Figure S2: Gating strategy used for the Flow Cytometry analysis. A. After gating on the lymphocytes via SSC-A/FSC-A cytograms, singlets were selected by FSC-H/FSC-A. The Live/Dead staining allowed selection of only live cells and the Dump channel to selected the $CD3^{-}CD14^{-}$ cells. **B.** Finally, CD56/CD16 markers identified NK cell subsets. Representative cytograms shown with gating based on FMO controls.

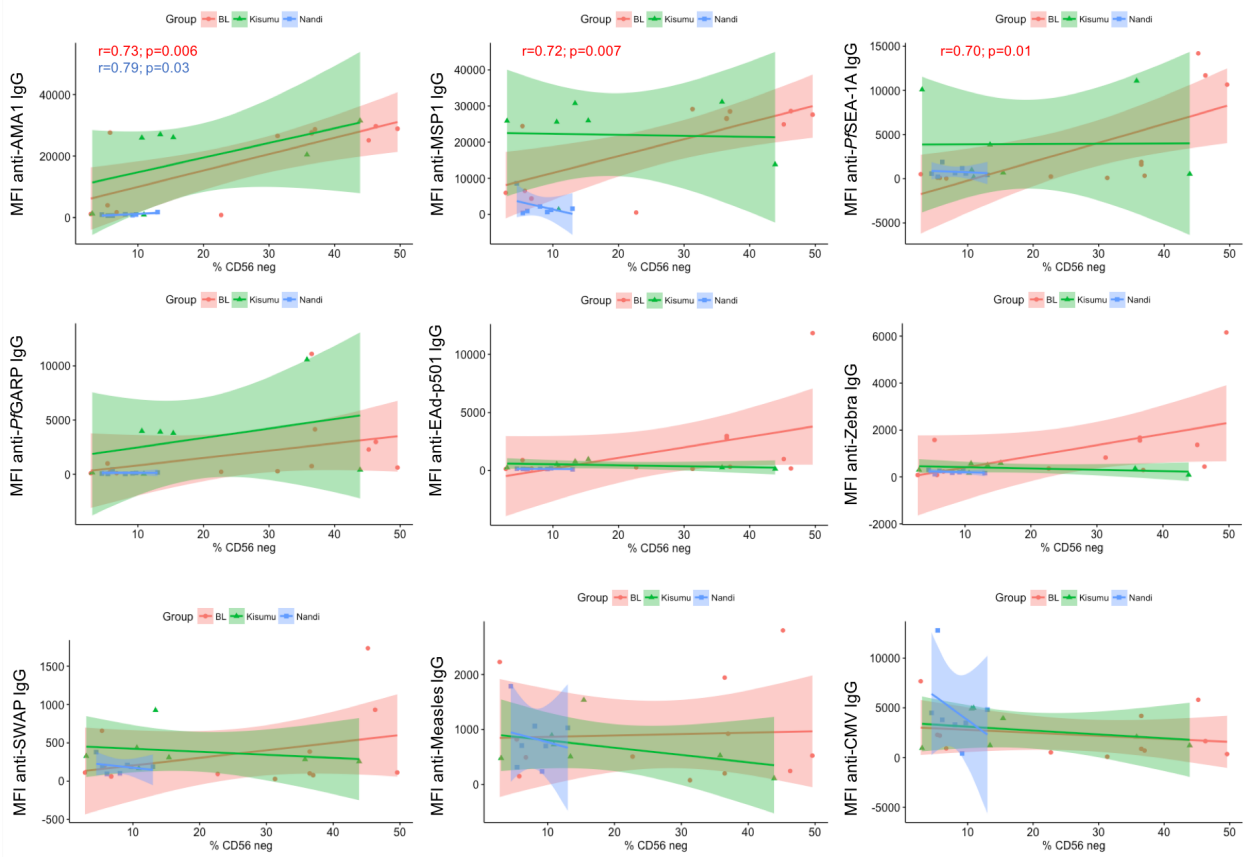

Figure S3: Correlation between the percentage of CD56^{neg}CD16^{pos} NK cells in our study populations and IgG antibody levels against malaria (AMA1, MSP1, r*Pf*-SEA-1A and *Pf*-GARB), EBV (Ead-p501 and Zebra), Schistosomiasis (SWAP), Measles and CMV (pp65). The correlation coefficient (r) and p-value for each group of children (n=7 Nandi in blue, n=7 Kisumu in green and n=12 eBL patients in red) is presented on each graph. Positive correlations were found for antibody levels against three malaria blood stage antigens, AMA1, MSP1 and PfSEA-1A and the frequencies of CD56^{neg}CD16^{pos} NK cells in eBL children.

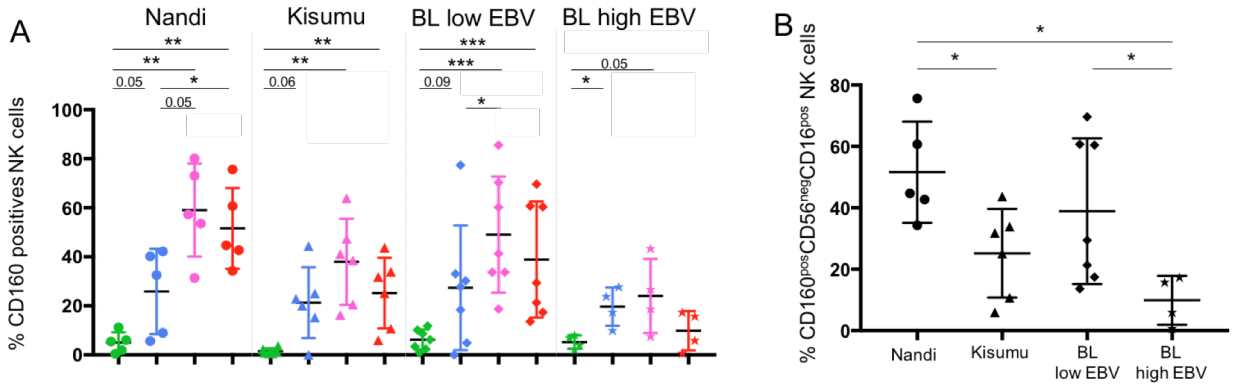

Figure S4: CD160 expression for different NK subsets across study groups of children. NK cell subsets defined as $CD56^{bright}CD16^{neg}$ (green), $CD56^{bright}CD16^{pos}$ (blue), $CD56^{dim}CD16^{pos}$ (pink) and $CD56^{neg}CD16^{pos}$ (red). Nandi (EBV^{low}/$Malaria^{low}$), Kisumu (EBV^{high}/$Malaria^{high}$) and eBL children with high and low EBV. (Nandi n=5; Kisumu n=6 and BL n=11). Comparison of CD160 **(A)** between different NK subsets within each group of children, and **(B)** focusing the $CD56^{neg}CD16^{pos}$ NK subset across study groups. Mann-Whitney statistical test (*p<0.05; **p<0.01; ***p<0.001).

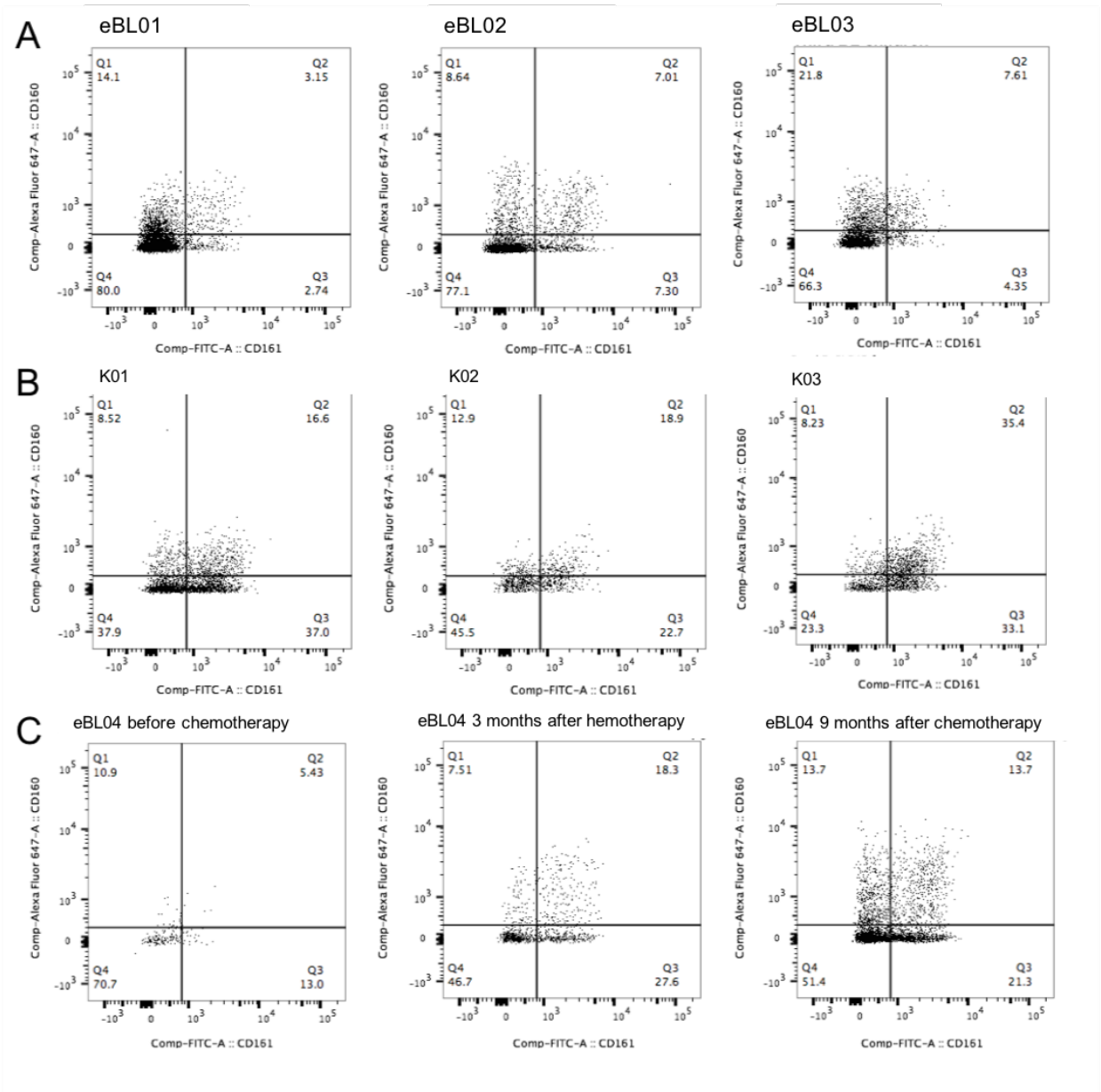

Figure S5: CD160 and CD161 co-expression for the CD56^{neg}CD16^{pos} subset. Representative histograms from three randomly selected **A**. eBL patients and **B.** healthy Kisumu children**.** Row **C** shows expression patterns from one eBL patient before induction of chemotherapy, and 3- and 9-months after completion of chemotherapy**.**

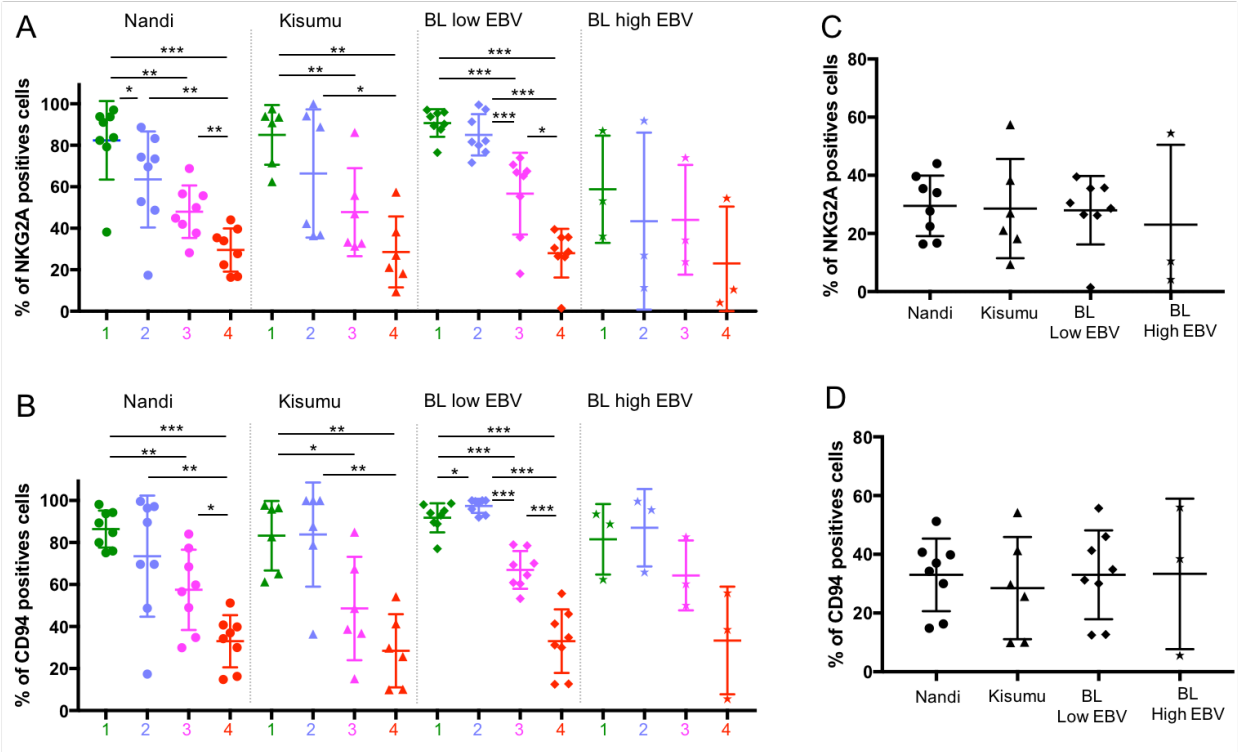

Figure S6: CD94 and NKG2A expression for different NK subsets across study populations. NK cell subsets defined as $CD56^{bright}CD16^{neg}$ (green), $CD56^{bright}CD16^{pos}$ (blue), $CD56^{dim}CD16^{pos}$ (pink) and $CD56^{neg}CD16^{pos}$ (red). Nandi (EBV^{low}/$Malaria^{low}$), Kisumu (EBV^{high}/$Malaria^{high}$) and eBL children with high and low EBV. (Nandi n=8; Kisumu n=6 and BL n=11). Comparisons of **A.** NKG2A and **B.** CD94 expression between the different NK subsets from all groups of children. Focusing on the expression of **C**. NKG2A and **D.** CD94 for the $CD56^{neg}CD16^{pos}$ NK subset and comparisons across study populations. Mann-Whitney statistical test (n.s = non significant; *p<0.05; **p<0.01; ***p<0.001).

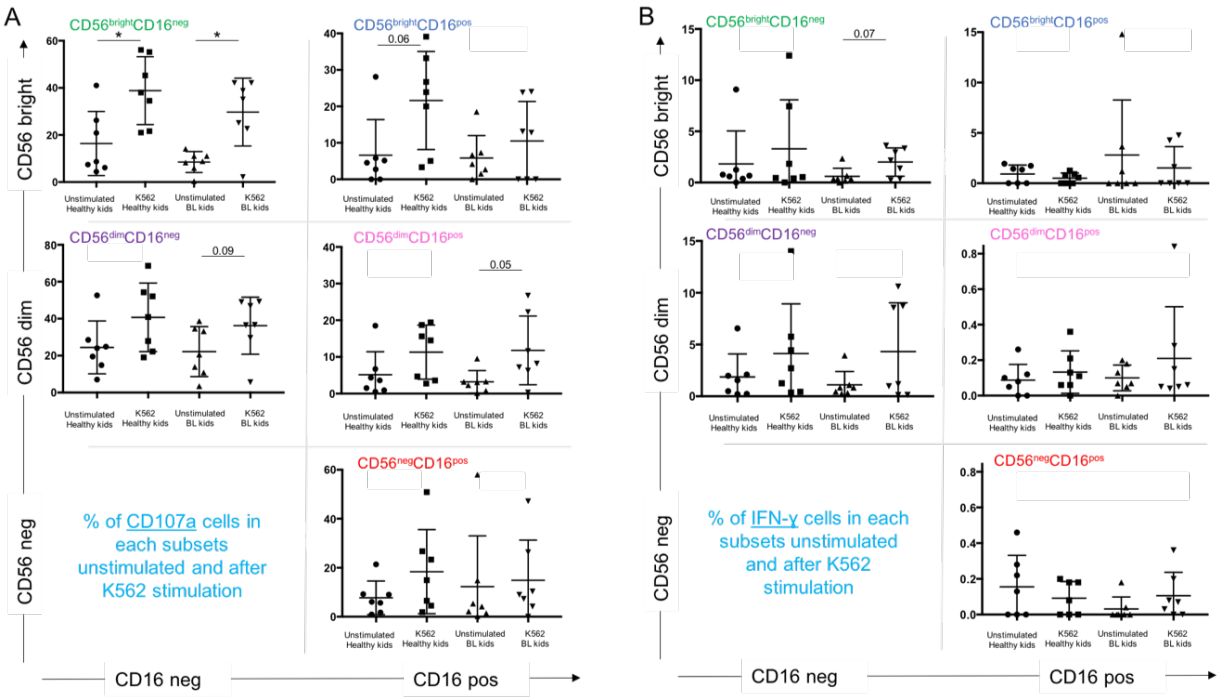

Figure S7: IFN-γ expression and CD107a degranulation of each NK cell subsets after K562 stimulation comparing healthy and eBL children. PBMCs from healthy (Nandi and Kisumu) and BL children were stimulated with K562 cell line and compared to unstimulated controls. NK cell subsets defined as $CD56^{bright}CD16^{neg}$ (green), $CD56^{bright}CD16^{pos}$ (blue), $CD56^{dim}CD16^{pos}$ (pink) and $CD56^{neg}CD16^{pos}$ (red). (Healthy kids n=7 and BL n=7). **A.** Percentage of CD107a positive NK cells within each subset with and without stimulation by K562. **B.** Percentage of IFN-γ positives NK cells within each subset with and without stimulation by K562. Wilcoxon statistical compared stimulated to unstimulated cells (n.s = non significant; *p<0.05).

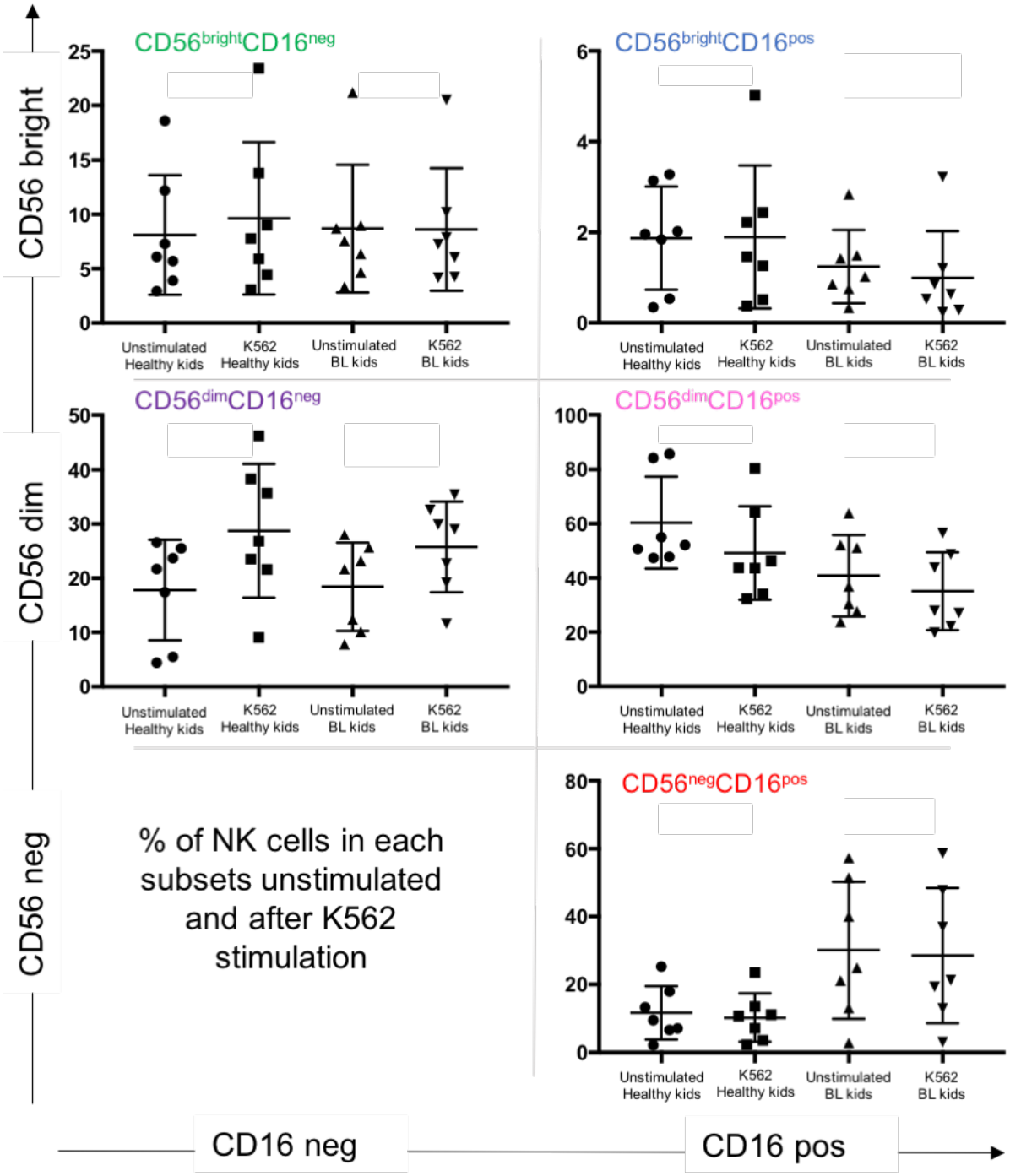

Figure S8: Proportion of NK subsets after K562 stimulation for healthy and eBL children. PBMCs from healthy (Nandi and Kisumu) and BL children were stimulated with K562 cell line and compared to unstimulated controls. NK cell subsets defined as $CD56^{bright}CD16^{neg}$ (green), $CD56^{bright}CD16^{pos}$ (blue), $CD56^{dim}CD16^{pos}$ (pink) and $CD56^{neg}CD16^{pos}$ (red). (Healthy children n=7 and BL n=7). Mann-Whitney statistical test shows no shift in NK subset proportions after K562 stimulation (n.s = non significant).

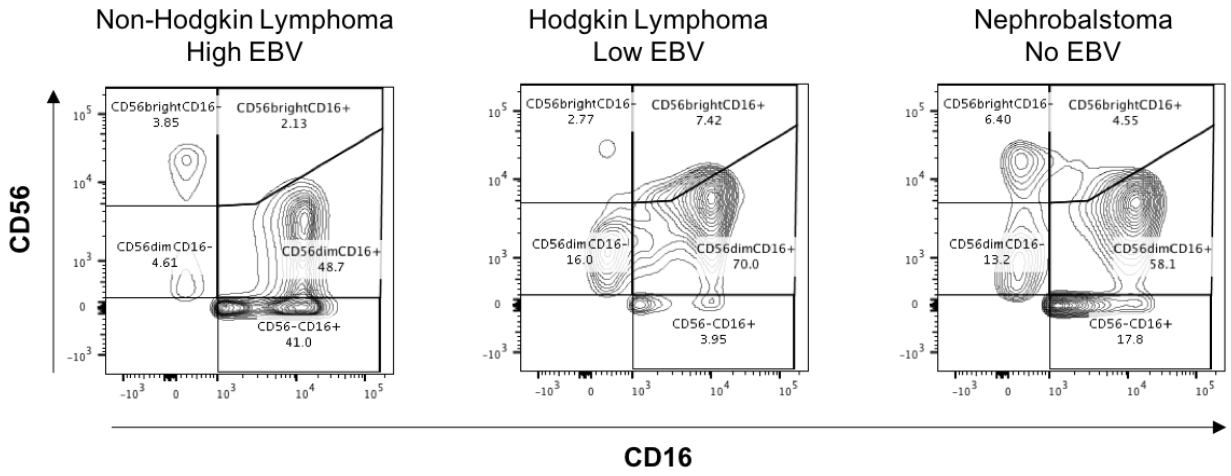

Figure S9: CD56^{neg}CD16^{pos} NK cell subset distribution in Kenyan children diagnosed with cancers other than eBL. Using the identical gating strategy explained in supplemental figure 2 for eBL patients, NK cell subset proportions were evaluated for three Kenyan children diagnosed with cancers other than eBL. The child with non-Hodgkin lymphoma who had a high EBV load showed a similar accumulation of the CD56^{neg} subset as found in eBL patients (Figure 1). In contrast, children diagnosed with Hodgkin lymphoma and nephroblastoma with low/no detectable EBV had NK cell subset proportions similar to healthy children, without and with malaria, respectively. This preliminary observation implicates EBV in driving NK cell subset skewing in cancer patients, however this provocative finding is cautiously interpreted due to the small sample size.

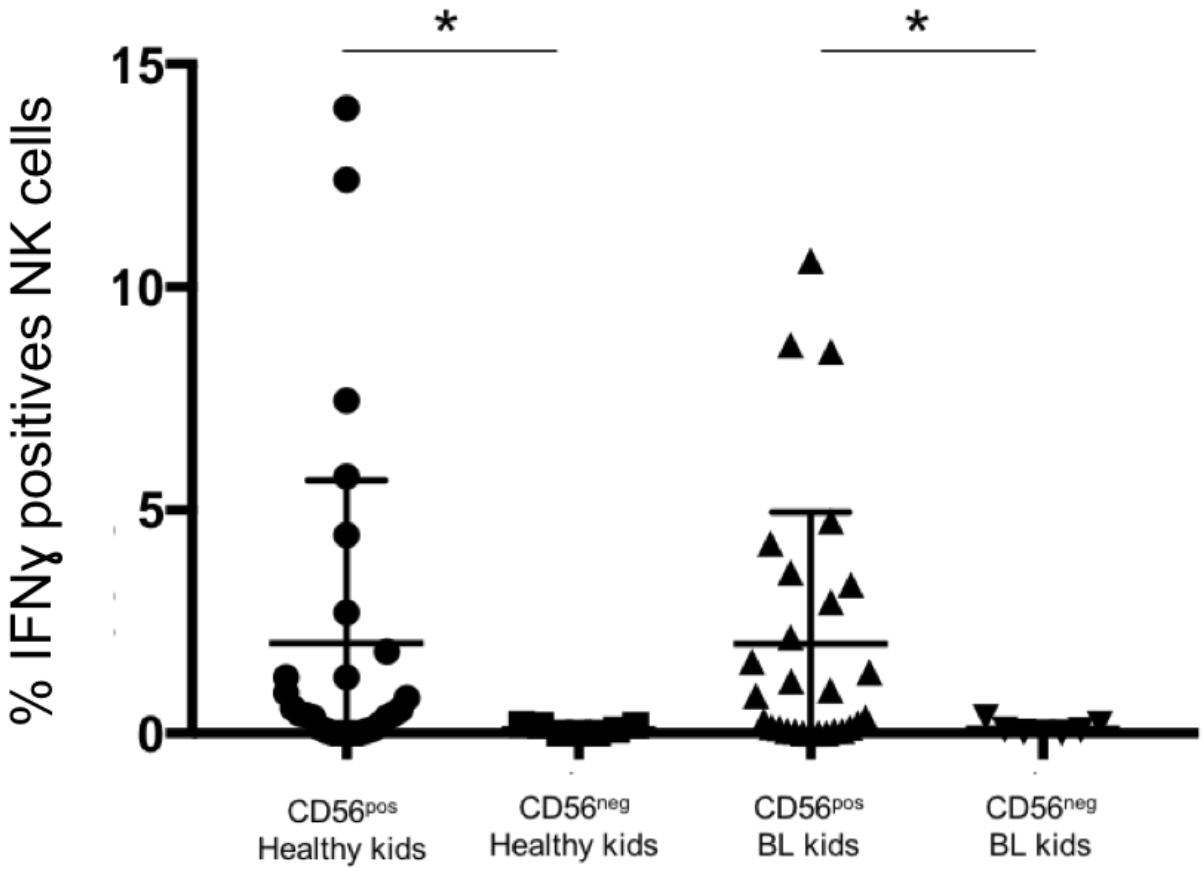

Figure S10: IFN-γ expression by CD56pos compared to CD56neg NK cells after K562 stimulation for healthy and eBL children. PBMCs from healthy (Nandi and Kisumu) and BL children were stimulated with K562 cell line and compared to unstimulated controls. (Healthy kids n=7 and BL n=7). Mann-Whitney statistical test comparing NK cells stratified by CD56 expression clearly demonstrates IFN-γ expression from CD56pos NK cells (*$p<0.05$) with no differences between healthy and eBL children for this cytokine.

References

1. Cosgrove C, Berger CT, Kroy DC, et al. Chronic HCV infection affects the NK cell phenotype in the blood more than in the liver. *PLoS One*. 2014;9(8):e105950.
2. Kimura H, Morita M, Yabuta Y, et al. Quantitative analysis of Epstein-Barr virus load by using a real-time PCR assay. *J. Clin. Microbiol.* 1999;37(1):132–136.
3. Moormann AM, Chelimo K, Sumba OP, et al. Exposure to holoendemic malaria results in elevated Epstein-Barr virus loads in children. *J. Infect. Dis.* 2005;191(8):1233–1238.
4. Mulama DH, Bailey JA, Foley J, et al. Sickle cell trait is not associated with endemic Burkitt lymphoma: an ethnicity and malaria endemicity-matched case-control study suggests factors controlling EBV may serve as a predictive biomarker for this pediatric cancer. *Int. J. Cancer*. 2014;134(3):645–653.
5. Fachiroh J, Paramita DK, Hariwiyanto B, et al. Single-assay combination of Epstein-Barr Virus (EBV) EBNA1-and viral capsid antigen-p18-derived synthetic peptides for measuring anti-EBV immunoglobulin G (IgG) and IgA antibody levels in sera from nasopharyngeal carcinoma patients: options for field screening. *J. Clin. Microbiol.* 2006;44(4):1459–1467.
6. Middeldorp JM, Herbrink P. Epstein-Barr virus specific marker molecules for early diagnosis of infectious mononucleosis. *J. Virol. Methods*. 1988;21(1-4):133–146.
7. van Grunsven WM, Spaan WJ, Middeldorp JM. Localization and diagnostic application of immunodominant domains of the BFRF3-encoded Epstein-Barr virus capsid protein. *J. Infect. Dis.* 1994;170(1):13–19.
8. Raj DK, Nixon CP, Nixon CE, et al. Antibodies to PfSEA-1 block parasite egress from RBCs and protect against malaria infection. *Science*. 2014;344(6186):871–877.
9. Cham GKK, Turner L, Lusingu J, et al. Sequential, ordered acquisition of antibodies to Plasmodium falciparum erythrocyte membrane protein 1 domains. *J. Immunol.* 2009;183(5):3356–3363.